MOLECULAR AND CELLULAR BIOLOGY, May 1996, p. 1966–1977 Vol. 16, No. 5
0270-7306/96/$04.00+0
Copyright © 1996, American Society for Microbiology

# Cytoplasmic Dynein (*ddlc1*) Mutations Cause Morphogenetic Defects and Apoptotic Cell Death in *Drosophila melanogaster*

THOMAS DICK,[1] KRISHANU RAY,[1] HELEN K. SALZ,[2] AND WILLIAM CHIA[1]*

*Institute of Molecular and Cell Biology, National University of Singapore, Singapore 0511, Republic of Singapore,[1] and Department of Genetics, Case Western Reserve University, Cleveland, Ohio 44106-4955[2]*

Received 5 September 1995/Returned for modification 31 October 1995/Accepted 6 February 1996

**We report the molecular and genetic characterization of the cytoplasmic dynein light-chain gene, *ddlc1*, from *Drosophila melanogaster*. *ddlc1* encodes the first cytoplasmic dynein light chain identified, and its genetic analysis represents the first in vivo characterization of cytoplasmic dynein function in higher eucaryotes. The *ddlc1* gene maps to 4E1-2 and encodes an 89-amino-acid polypeptide with a high similarity to the axonemal 8-kDa outer-arm dynein light chain from *Chlamydomonas* flagella. Developmental Northern (RNA) blot analysis and ovary and embryo RNA in situ hybridizations indicate that the *ddlc1* gene is expressed ubiquitously. Anti-DDLC1 antibody analyses show that the DDLC1 protein is localized in the cytoplasm. P-element-induced partial-loss-of-function mutations cause pleiotropic morphogenetic defects in bristle and wing development, as well as in oogenesis, and hence result in female sterility. The morphological abnormalities found in the ovaries are always associated with a loss of cellular shape and structure, as visualized by a disorganization of the actin cytoskeleton. Total-loss-of-function mutations cause lethality. A large proportion of mutant animals degenerate during embryogenesis, and the dying cells show morphological changes characteristic of apoptosis, namely, cell and nuclear condensation and fragmentation, as well as DNA degradation. Cloning of the human homolog of the *ddlc1* gene, *hdlc1*, demonstrates that the dynein light-chain 1 is highly conserved in flies and humans. Northern blot analysis and epitope tagging show that the *hdlc1* gene is ubiquitously expressed and that the human dynein light chain 1 is localized in the cytoplasm. *hdlc1* maps to 14q24.**

Dyneins are molecular motors that translocate along microtubules. Originally, dyneins were identified in eucaryotic axonemes as the ATPase required for flagellar and ciliary beating (10). Later, cytoplasmic forms of the enzyme were isolated (26).

While the role of axonemal dynein in mediating flagellar and ciliary beating seems reasonably clear, the extent of cellular functions involving cytoplasmic dynein has yet to be fully defined. This molecular complex is thought to be responsible for the retrograde directed transport of organelles within the cell, including axonal transport, as well as for the centripetal transport of endosomes, lysosomes, and the elements of the Golgi apparatus in cells in general. However, there is evidence that also points to a role of cytoplasmic dynein in mitosis (see references 14 and 42 for reviews). Because of the lack of mutations in any cytoplasmic dynein subunit in higher eucaryotes, the in vivo functions of the enzyme are little understood.

Cytoplasmic dyneins are large enzyme complexes with a molecular mass of about 1,200 kDa and contain two force-producing heads (43). The heads are thought to be formed primarily from the heavy chains, large, apparently identical polypeptides responsible for ATP hydrolysis. Stalks link the heads to a basal domain, which is less well defined and contains a varying number of accessory intermediate chains (see reference 14 for a review). The intermediate chains are thought to play a role in targeting the enzyme complex within the cell. They might be involved in linking the enzyme to the surface of various membranous organelles, kinetochores, or other cellular cargoes and targets (25). Identifying all the components of the cytoplasmic dyneins is a prerequisite to elucidating their structural organization and mechanism of action.

Recently, the gene encoding the cytoplasmic dynein heavy chain from *Drosophila melanogaster* was cloned (20, 29) and the distribution of its transcript and protein was analyzed (13, 20). The expression of the gene is essentially ubiquitous. The dynein heavy-chain protein is associated with several microtubule arrays. Interestingly, within the developing egg chamber of the ovary, the cytoplasmic dynein heavy-chain gene is transcribed predominantly in the nurse cells. In contrast, the encoded protein displays a striking accumulation in the oocyte, suggesting that cytoplasmic dynein is maternally transported from the nurse cells into the developing oocyte (20).

*Drosophila* oogenesis is very sensitive to mutations that affect fundamental cell biological processes, and many mutations of important cellular genes are known to interfere with the proper development of the egg, causing female sterility (see, e.g., reference 7 for a review on cytoskeletal genes). Hence, female sterile mutations are potentially a rich source of these important genes. More than 1,300 female sterile mutations in *D. melanogaster* are known. Half of these mutants are thought to be partial-loss-of-function alleles of vital genes (27, 34).

We report here the molecular and genetic characterization of a *Drosophila* female sterile mutation mapping to 4E1-2 on the X chromosome. We show that the mutation is a partial-loss-of-function allele of a gene encoding the cytoplasmic homolog of the axonemal 8-kDa outer-arm dynein light chain from *Chlamydomonas reinhardtii*. We named the gene *ddlc1* (*Drosophila* dynein light-chain 1). DDLC1 is the first cytoplasmic dynein light chain identified, and the female sterile *ddlc1* mutation is the first mutation in a cytoplasmic dynein subunit in higher eucaryotes. We describe the pleiotropic defects in

* Corresponding author. Mailing address: Institute of Molecular and Cell Biology, National University of Singapore, 10 Kent Ridge Crescent, Singapore 0511, Republic of Singapore. Phone: (65) 7723790. Fax: (65) 7791117. Electronic mail address: MCBWCHIA@LEONIS.NUS.SG.

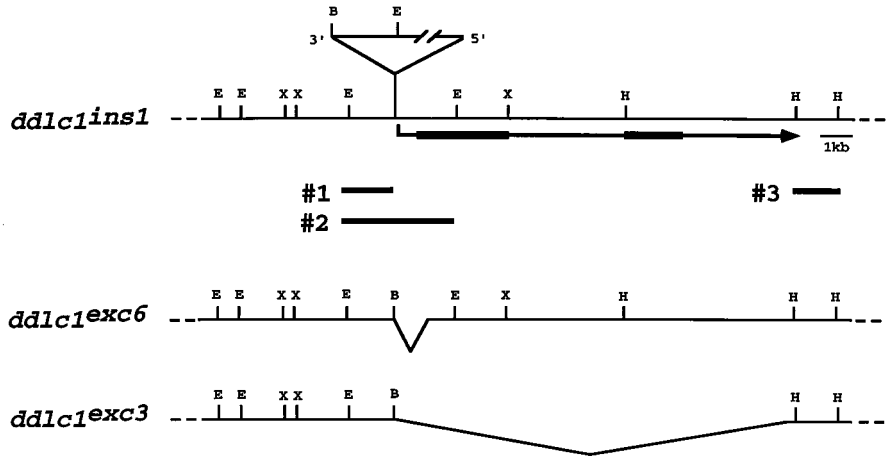


FIG. 1. Genomic region encompassing the *ddlc1* gene. A restriction map of the genomic DNA is shown. The extent of the major, 2.4-kb *ddlc1* transcript and its direction of transcription are indicated by a horizontal arrow; however, the precise intron-exon organization has not been elucidated. Northern blot analyses with various genomic fragments show that the developmentally regulated 4.5-kb mRNA covers the same genomic region that is indicated by the arrow for the major 2.4-kb transcript and extents further downstream. The genomic 1.1-kb *Hin*dIII fragment immediately downstream of the arrowhead (fragment 3) hybridizes specifically to the 4.5-kb but not to the 2.4-kb transcript (see Materials and Methods). The inverted broken triangle represents the P-element insertion site in the *ddlc1* allele $ddlc1^{ins1}$. Its position of insertion (≈40 bp upstream of the 2.4-kb transcription unit) was determined by sequencing the genomic DNA. #1 indicates the 1.5-kb flanking DNA fragment cloned from genomic DNA prepared from the insertion line (see Materials and Methods). #2 indicates the genomic fragment used for cloning the cDNAs representing the 2.4-kb transcript. The deleted sequences in the recessive lethal excision alleles $ddlc1^{exc6}$ and $ddlc1^{exc3}$ are indicated. The two intervals to which the coding region of the major, 2.4-kb mRNA was mapped are indicated by bars on the arrow that indicates the 2.4-kb transcription unit. $ddlc1^{exc3}$ deletes the whole *ddlc1* 2.4-kb mRNA coding region. Whether $ddlc1^{exc6}$ deletes into the coding sequence or removes only the 5′ transcribed but untranslated region has not been determined. E, *Eco*RI; X, *Xho*I; B, *Bam*HI; H, *Hin*dIII.

oogenesis and wing and bristle morphology caused by the original, partial-loss-of-function *ddlc1* mutation, as well as the embryonic phenotype of total-loss-of-function *ddlc1* alleles. Furthermore, the cloning, expression pattern, and chromosome mapping of the human homolog, *hdlc1*, are reported, demonstrating that the dynein light chain 1 is highly conserved in flies and humans.

## MATERIALS AND METHODS

Standard molecular biology techniques were carried out as described by Sambrook et al. (33). Standard fly manipulation techniques were performed as described by Ashburner (1).

**Strains.** The P[w+]4E1-2 insertion strain ($ddlc1^{ins1}$) was isolated in a female sterile screen (32). It contains a P-lacW (3) insertion at 4E1-2. The transposable portion of P-lacW is 10.6 kb long and contains a plasmid origin of replication and the β-lactamase gene at its 3′ end. The plasmid sequences are bounded by two linker sequences containing an *Eco*RI site in one and a *Bam*HI site in the other (Fig. 1). The FM7c chromosome used throughout in this report contained a dominant marker (a *lacZ* gene driven by the *ftz* promoter), which facilitates the identification of homozygous mutant embryos. Details of balancer strains are given by Lindsley and Zimm (21).

**Isolation of *ddlc1* genomic and cDNAs.** Genomic DNA flanking the P-lacW insertion site was cloned by the plasmid rescue technique. Fly genomic DNA was prepared from the P-lacW insertion line $ddlc1^{ins1}$. The DNA was digested with *Eco*RI, ligated, and transformed into *Escherichia coli*. Colonies containing the plasmid sequence of the P-lacW element with flanking genomic DNA were picked. The rescued plasmid was digested with *Eco*RI and *Bam*HI to isolate a 1.5-kb DNA fragment flanking the P-element insertion site (fragment 1, Fig. 1). The flanking DNA was used as a probe to screen an EMBL3 wild-type genomic library (40). Genomic fragment 2 (Fig. 1), which surrounds the P-lacW insertion site, was used to screen a 4- to 8-h embryonic cDNA library constructed by Brown and Kafatos (4).

**Northern blot analysis.** Fly poly(A)$^+$ RNA was prepared by standard methods. RNA samples (2 μg) were separated on formaldehyde-agarose gels and were transferred to nylon membranes, hybridized, and exposed as described by Sambrook et al. (33). The human multiple-tissue Northern (RNA) blot was obtained from Clontech. The genomic *ddlc1* fragments used as probes to characterize the relationship between the *ddlc1* gene and its 2.4- and 4.5-kb transcripts, respectively, were (Fig. 1) fragment 1, fragment 2, 1.5-kb *Eco*RI-*Xho*I, 3.5-kb *Xho*I-*Hin*dIII, 5.3-kb *Hin*dIII-*Hin*dIII, and 1.1-kb *Hin*dIII-*Hin*dIII (fragment 3). Fragment 1 did not hybridize to the two transcripts, and fragment 3 hybridized specifically to the 4.5-kb mRNA. The internal 3.5-kb *Xho*I-*Hin*dIII fragment did not hybridize to the two mRNAs, indicating the presence of an intron spanning that genomic region. The other fragments hybridized to both transcripts. These results suggest that (i) the *ddlc1* transcription unit is localized on the right side of the $ddlc1^{ins1}$ P-element insertion (Fig. 1); (ii) both transcripts have their start points in the genomic sequence between the P-element insertion site and the *Eco*RI site 1.8 kb to the right of it; and (iii) the 4.5-kb mRNA extends further downstream than the 2.4-kb mRNA. The DNA fragments from the 2.3-kb cDNA (representing the 2.4-kb mRNA) used as probes to characterize the relationship between the 2.4-kb mRNA and the 4.5-kb mRNA were, from 5′ to 3′ (accession number U32855), 0.45-kb [*Hin*dIII]-*Pvu*II, 0.48-kb *Pvu*II-*Pvu*II, 0.4-kb *Pvu*II-*Pvu*II, and 1-kb *Pvu*II-[*Pvu*II], where brackets indicate restriction sites in the polylinker. All cDNA fragments hybridized to both the 2.4- and the 4.5-kb mRNAs.

**DNA sequencing.** Overlapping restriction fragments were subcloned into M13 and Bluescript and sequenced with universal and gene specific primers. Sequences were assembled and analyzed with DNA Star software. Databases were searched by using BLAST at the National Center for Biotechnology Information, National Institutes of Health.

**Whole-mount embryo and ovary RNA in situ hybridization.** *Drosophila* embryos were collected, fixed, and hybridized as described previously (41), with PCR-generated digoxigenin-labelled probes (Boehringer Mannheim). Anti-digoxigenin-horseradish peroxidase antibody was used to detect the hybridized probe. Whole-mount in situ hybridization to ovaries was performed by the method of Cooley et al. (8).

**Immunocytochemistry.** Anti-DDLC1 antibody was raised in mice by immunization with the 19-mer peptide KDIAAYIKKEFDKKYNPTW conjugated to diphtheria toxoid (Chiron). The embryos and ovaries were stained by following standard protocols as described by Ashburner (1). The embryos were collected, dechorionated, treated with 10 mM taxol (Sigma Co.) in 0.1 M piperazine-*N*,*N*′-bis-(2-ethanesulfonic acid) (PIPES; pH 6.9)–2 mM ethylene glycol-bis(β-amino-ethyl ether)-*N*,*N*,*N*′,*N*′-tetraacetic acid (EGTA)–1 mM $MgSO_4$ for 5 min in a buffer-heptane interface, and fixed for 40 min by adding 35% formaldehyde to a final concentration of 4%. The vitelline membrane was removed by shaking the embryos repeatedly in 80% ethanol–heptane. The embryos were rehydrated in phosphate-buffered saline (PBS), preincubated for 1 h, with blocking solution containing 3% bovine serum albumin and 0.1% Triton X-100 in PBS, and then incubated overnight at 4°C with the corresponding antiserum. The serum dilutions used were as follows: mouse anti-DDLC1 serum, 1:1,000; rat anti-tubulin, 1:20; and rabbit anti-β-galactosidase (Cappel Inc.) 1:5,000. The antibody binding to the tissue was visualized with specific antisera raised against the F(ab) fragment of the mouse, rat, and rabbit, respectively. Both fluorescein isothiocyanate-conjugated and horseradish peroxidase-conjugated secondary antisera were used. The ovaries were dissected and treated similarly to the embryos and then fixed and stained as described above.

**Nuclear and cytoskeletal staining of embryos and ovaries.** Embryos were collected and fixed as previously described (48). For DNA staining with YPRO-I, the embryos were incubated with 100 μg of RNase A per ml in PBS–0.1% Triton

X-100 (PBT) for 1 h, washed several times in PBT, incubated with 1 μg of YPRO-I (Molecular Probes Inc.) per ml in PBT for 1 h, and washed before being mounted. DNA fragmentation in embryos was analyzed by TUNEL staining (44). The embryos were fixed, washed in PBT, and incubated for 3 h at 37°C with terminal transferase and biotin-dUTP (Boehringer Mannheim). The reaction was stopped by washing in PBT, and the embryos were incubated with 20 μg of avidin-fluorescein isothiocyonate per ml for 1 h. The embryos were counterstained with Texas red (XTRITC; 3 μg/ml)-conjugated phalloidin (Sigma Chemical Co.) for 30 min, washed, and mounted in a drop of Vectashield (Vector Labs Inc.). The ovaries were dissected from the adult females and fixed in 4% formaldehyde in PBS for 40 min. After several washes in PBT, the ovaries were incubated with Texas red-conjugated phalloidin–0.5 μg of 4′,6-diamidino-2-phenylindole (DAPI) (Sigma Chemical Co.) per ml in PBT for 1 h. The embryos were washed in PBT and mounted with a drop of Vectashield. The stainings were observed by using the epifluorescence setup in a Zeiss Axioplan microscope, and the images were recorded with a STAR1-cooled charge-coupled device (CCD) camera and a Macintosh Q900 computer. The images were further processed with Adobe Photoshop 2.01 and either printed in a Phaser IIXD dyesub printer or exposed on a photographic film with an Agfa PCRII camera. For better resolution, some of the pictures were taken with a Bio-Rad laser-scanning confocal microscope, MRC 600, and then processed and printed as above.

**Generation of *ddlc1* alleles by P-element mobilization and genetic mapping of the *ddlc1* allelels.** To generate deletion mutations in the *ddlc1* gene, the P-element ($ddlc1^{ins1}$) inserted ≈40 bp upstream of the *ddlc1* transcription unit was mobilized, as described previously (30), and imprecise excisions that affect the *ddlc1* transcription unit were generated. Females heterozygous for the P-element insertion ($ddlc1^{ins1}$/FM7c) were crossed to males carrying the Sb P[Δ2-3](99B) element. Progeny jump-starter males containing the $ddlc1^{ins1}$ chromosome and Sb P[Δ2-3](99B) were mated to FM7c/FM7c females. Female progeny were scored for loss of the P-lacW insertion and crossed to FM7c/Y males. In the case of a viable, fertile jumpout, males carrying the excision chromosome were crossed to excision/FM7c females and their progeny were mated to establish homozygous excision lines. In the case of lethal jumpouts, excision/FM7c females were crossed to FM7c/Y males and kept as balanced lines. Starting from 100 jump-starter crosses, 50 viable and fertile as well as 2 lethal jumpouts ($ddlc1^{exc3}$ and $ddlc1^{exc6}$) were obtained. Two P-element insertions ($ddlc1^{ins2}$ and $ddlc1^{ins3}$) were obtained from an independent screen for female sterile mutations in the 4E region. All *ddlc1* alleles were shown to belong to one complementation group. Furthermore, all *ddlc1* alleles were genetically mapped to the 4E1-2 region by using the deficiencies Df(1)ovoG6 (4C11-12;4F1,2), Df(1)svbEH (cytology not visible [$hnt^-$, $svb^-$, $ovo^-$]), and Df(1)DEB4D (4E1,2;4F11-12) (31). The last two deficiencies coming from the left and right side of 4E, respectively, both break within the 4E1-2 region but do not overlap. The deletion present in Df(1)ovoG6 includes 4E1-2. All *ddlc1* alleles failed to complement Df(1)ovoG6 while they were viable and fertile over the Df(1)svbEH and Df(1)DEB4D. Hence, the lesions causing lethality and female sterility are placed in the region between the right breakpoint of Df(1)svbEH and the left breakpoint of Df(1)DEB4D at 4E1-2. The fertility of the *ddlc1* P-element insertion alleles over the Df(1)svbEH (which deletes the *ovo* gene) indicates that the sterility caused by the homozygous *ddlc1* P-element insertions is unrelated to the *ovo* gene.

**Isolation of *hdlc1* cDNAs.** PCR was carried out for 35 cycles (of 95, 60, and 72°C, each for 1 min) with 100 ng of cDNA template from the HUT-78 T-cell cDNA library (Clontech). The oligonucleotide primers (containing *Not*I linkers) used were hPCRI (AAGCGGCCGCGACAGGAAGGCCGTGATCAAGAAC GC) and hPCRII (TTGCGGCCGCTTGAACAGCAGGATGGCCACCTGGC C). One-tenth of the reaction mixture was digested with *Not*I, and the expected 300-bp fragment was isolated by electrophoresis and cloned into Bluescript. The cloned PCR fragment was used to screen the lambda gt11 HUT-78 cDNA library.

**Chromosome mapping of the *hdlc1* gene.** The *hdlc1* cDNA was used as a probe to isolate the human P1 clone F0819. DNA from F0819 was labeled with biotin dUTP by nick translation and hybridized to normal metaphase chromosomes derived from lymphocytes. Specific hybridization signals were detected by incubating the hybridized slides in fluoresceinated avidin. Following signal detection, the slides were counterstained with propidium iodide and analyzed. This experiment resulted in specific labelling of the long arm of a group D chromosome. To confirm the identity of the specifically labelled chromosome, clone F0819 was cohybridized with a chromosome 14 centromere-specific probe. This experiment demonstrated that F0819 hybridizes to chromosome 14. Measurement of 10 specifically hybridized chromosomes 14 showed that F0819 is located 68% of the distance from the centromere to the telomere of chromosome arm 14q, an area that corresponds to band 14q24. A total of 80 metaphase cells were analyzed, and 74 exhibited specific labelling (BIOS Laboratories, Inc., Connecticut).

**myc tagging and cell culture.** Cos cells were grown in Dulbecco minimal essential medium supplemented with 10% fetal bovine serum. The plasmids for transfection of the myc-tagged *hdlc1* gene were constructed as follows. The vector pXJ41 (a gift from the Hong Wanjin laboratory) containing the human cytomegalovirus promoter, was cut with *Eco*RI and *Bam*HI. By using PCR, two *Eco*RI-*Bam*HI *hdlc1* fragments, containing an N-terminal and a C-terminal myc tag, respectively, were generated. The myc-hdlc1 fragments were inserted downstream of the human cytomegalovirus promoter, resulting in plasmids p-Nmyc-hdlc1 and p-Cmyc-hdlc1, respectively. The two primer pairs used for PCR were

A

```
GAGTTAATCACCAGCAAGCAAAACGTTCAGTTGTGTTACAGTTGTCGAGAAGTCAGGGTG    60
TTTCTACCTTCCATTTACCGTTCCAGCGTAAAATTCAGGCGACACGCTTAGCGGTAAAAA   120
ACCCACACATCCACGCACAATAAAGTATATTGGGGCAAATGTTTTTTCAACCCGGTTCCT   180
AGAGATCTTCTGAAAAAACAATTCCCTATCTACTGTTCTTTTTTTCTCGTTCTCTGTTCT   240
CAAAGTGAAGTAGCCGCGGCGTGCTAAATTTGTATTGCGTGCAAAATTGTTAAAAAAAAA   300
AAGAAACCGAAAGAGAAATAAGCAAACACATACACACGCATTCCGCATTTTTCCTGCCCA   360
CAACTTTTTTTTTTGAAAGTTCAAATTTGGTATTGCATTAGAATTTATTTGGTGACAGCT   420
GTTGAACTATGAGTGAAAAAATCGCGCGCAATCAGGAAAAATTAAAAGTTACCAAGGAGA   480
ACCGCTAAAAAGGGCCACTTTTCAAACGGTTAGATTCCAGTGAAGTTGTAAGCACACAGG   540
GAACCTAAAAAAAAAAAAAAAAAAAGCCAAAATGTCTGATCGCAAGGCCGTGATTAAAAAT   600
                          M  S  D  R  K  A  V  I  K  N
GCCGACATGAGCGAGGAGATGCAGCAGGATGCCGTCGATTGTGCGACACAGGCCCTCGAG   660
 A  D  M  S  E  E  M  Q  Q  D  A  V  D  C  A  T  Q  A  L  E
AAGTACAACATTGAAAAGGACATTGCGGCCTACATCAAGAAGGAGTTCGACAAAAAATAC   720
 K  Y  N  I  E  K  D  I  A  A  Y  I  K  K  E  F  D  K  K  Y
AATCCCACATGGCATTGCATTGTCGGTCGCAACTTTGGATCGTATGTCACACACGAGACG   780
 N  P  T  W  H  C  I  V  G  R  N  F  G  S  Y  V  T  H  E  T
CGCCACTTTATTTACTTCTATTTGGGCCAGGTGGCTATTTTACTGTTTAAGAGCGGTTAA   840
 R  H  F  I  Y  F  Y  L  G  Q  V  A  I  L  L  F  K  S  G  *
AGTATTGTCGAGTCGGATGAAGTGGTGGTGAGGAGGCTGATGGAGATGCAGCAGCTGCCC   900
CGCCAGCAGCAACAACAGCAGGGGCAGCAGTCGCATTTCGGAGCATCAGAGGATGAGGAT   960
CTAGAGCAGAAACAGCAACAACCACAACAATCACAGCAACTACAGAGCCAGCAGCAACAA  1020
CAACAACAACAACAACAACAACAACAACAACAACAACTACAAAAAGAACAAGAACGAAAA  1080
CAGCAAACACTACAACCACCAGTAGAACATCTCAAGGATGCGGAAATGATGACCGATAGC  1140
GCAAGCGAGAAGCAACAGCAGCAAAAACGATCAGAAGATTCGCAAATACAACTAACCAAC  1200
GATCAAGACGTGGACGATGGGGACGAAGACGAAGACGAGGACGAGGACGATGAAGATGGC  1260
ACCATTGTGGAGGACAGCGATGCCACCAGCTGCAGCAGTTGTCGACGAGCCGAACTGGAG  1320
GATAATCAGCAAGAACAACCGCCGACATCATCATCTCCCCACAAGGATCGGGAACACGTC  1380
ACATAGGGCATTCTCTTTCACAATATGGAGAGAGAGGCTACACACGAGCACACCGTTCTA  1440
GATTGTCTATCGGATGCAAACAACGCCGATTGGTTGGTGGTACAGATTATATACAATATA  1500
TGCTCAGCAATTTAAATTGAACAAGCGTTGATGTTCAATAGGAAAGCGCTACTAGAACAC  1560
ACAAAATACACTACTAGAAACAGAGGAACTTGTTTAGAAGCACGAACCAACGATGTTTAG  1620
TTTCGAAATCACCATTTCCCGTCCTAAACTTCTGCATGTTGATGGTATAGTTTAGAATAA  1680
GCAATTGGTTACCATTTGGATTTGCATTCGCTCCCAATGATTCAAACATCTGTTGAAATA  1740
TACTTTTAATATTTTCTTTTGCAATGTTTATGGCTGGAGCTTGTTGGACTTTGATTACAT  1800
ATGAAACCTGCGCAATTAAACAATTGTTACAGAAAGAACCAAAACTATGTGTTATATTAT  1860
TTTCCATTTTTATTTTCAATCCAATTTCGTTGGCGCTTAGCAGAGGCAAGAACCACACAT  1920
ACACACACACACACACACACACACAAACACACACACACACGGACACGGACACATAGCA  1980
CAGGCAACAACCACCACTACAACCGAACGAGTAAAATAAAAAGAAAAACTGAATATTTAA  2040
CAAAATTGTAAGGAAAACTCACATATTTTTCTGTCGGATGGATTATTTATGTGTATTGAA  2100
CTCTCAACACTTGTAATCGGAAACCAAGCAGAAAGTATATAAAAAAAAATAGTATAATGT  2160
GAAATTTGCATACACACCATACTCACTCACACACACAGACGCTCTCTGCACACCTAATGG  2220
GTACACAGAGAAAAATATCTCATTGGCATGCTTTTCCC  2258
```

FIG. 2. Nucleotide sequence of the 2.4-kb *ddlc1* transcript, amino acid sequence of the deduced DDLC1 protein and sequence comparison of dynein light chains. (A) The nucleotide sequence of the 2.3-kb *ddlc1* cDNA is shown along with the deduced DDLC1 amino acid sequence. (B) The sequence of the predicted *D. melanogaster* DDLC1 protein, its homologs from *Caenorhabditis elegans* (CDLC1 [46]), humans (HDLC1 [this paper]), and the flagellar 8-kDa outer-arm dynein light chain from *C. reinhardtii* (O.A.DLC [17]) are shown. Amino acids identical to the *C. reinhardtii* dynein light chain are boxed.

AAGAATTCACCATGGAGCAGAAGCTGATCAGCGAGGAAGACCTG plus AAGGATCCTTAACCAGATTTGAACAGAAG and AAGAATTCAC CATGTGCGACCGAAAGGCC plus AAGGATCCTTACAGGTCTTCCTCG CTGATCAGCTTCTGCTC, respectively. Transfections and antibody probing were carried out as previously described (22).

**Nucleotide sequence accession numbers.** The nucleotide sequences reported in this paper have been submitted to the GenBank database under accession numbers U32855 (*ddlc1*) and U32944 (*hdlc1*).

## RESULTS

**Identification, cloning, and analysis of the *ddlc1* gene and three mutant alleles in *D. melanogaster*.** $ddlc1^{ins1}$ was identified from a screen of homozygous viable single P-element insertions that show recessive female sterility and mapped to 4E1-2 on the X chromosome (see Materials and Methods). Results from reversion experiments have shown that this P-element insertion is responsible for the female sterility. By using stan-

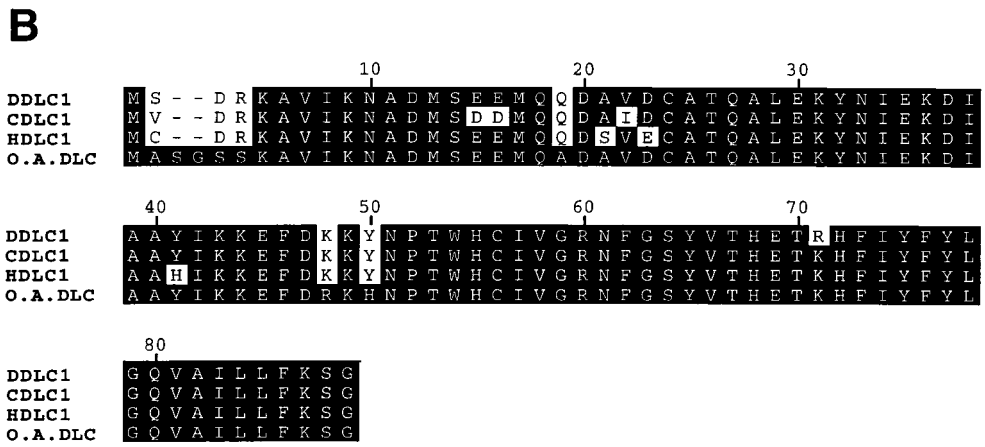


FIG. 2—*Continued.*

dard methods, 20 kb of genomic DNA flanking the *ddlc1*$^{ins1}$ P-element insertion was isolated. Within the cloned genomic region, a transcription unit encoding a major transcript of 2.4 kb was detected. Genomic high-stringency Southern blot analyses showed that the *ddlc1* gene is a single-copy gene. With the genomic DNA as a probe, cDNA clones from an early (4- to 8-h) embryonic library were obtained that encompassed the coding region of the 2.4-kb *ddlc1* transcript. The organization of the *ddlc1* transcription unit was determined by sequencing and Northern and Southern blotting. The P-element insertion site is localized approximately 40 bp upstream of the transcriptional start site of the 2.4-kb *ddlc1* mRNA. A schematic summary of the organization of the *ddlc1* transcription unit relative to the genomic DNA and the *ddlc1*$^{ins1}$ P-element insertion site is shown in Fig. 1. Developmental Northern blot analyses revealed that the *ddlc1* gene encodes a second, minor, developmentally regulated transcript of 4.5 kb (see Fig. 3A). A systematic Northern analysis with various genomic fragments as probes (see Fig. 1 legend and Materials and Methods for details) showed that the 4.5-kb transcript covers the same genomic region that is covered by the major, 2.4-kb transcript but extends further downstream. Northern analyses with various subfragments of the cDNA representing the major, 2.4-kb mRNA failed to detect a probe specific only for the 2.4-kb transcript (see Materials and Methods). This result suggests that most of the sequence of the 2.4-kb transcript is also present in the 4.5-kb mRNA. To generate total-loss-of-function alleles of *ddlc1*, we mobilized the original P-element *ddlc1*$^{ins1}$ and attempted to isolate imprecise excisions that removed the *ddlc1* gene. The mutations obtained were analyzed, and the structural defects associated with two of the alleles (*ddlc1*$^{exc6}$ and *ddlc1*$^{exc3}$) are schematically summarized in Fig. 1. The two *ddlc1* alleles that remove the *ddlc1* transcription unit encoding the major, 2.4-kb mRNA either partially (*ddlc1*$^{exc6}$) or completely (*ddlc1*$^{exc3}$) cause recessive lethality.

**The *ddlc1* gene product encoded by the major, 2.4-kb transcript is similar to the flagellar 8-kDa outer-arm dynein light chain from *C. reinhardtii*.** To isolate cDNAs representing the major, 2.4-kb *ddlc1* transcript, a 4- to 8-h embryonic library was screened. Since the developmentally regulated 4.5-kb mRNA is not detectable in early embryos (before 12 h [see Fig. 3A]), the resulting cDNA clones represent the 2.4-kb and not the 4.5-kb *ddlc1* mRNA. Six cDNAs covering the DDLC1 protein-coding region of the major, 2.4-kb transcript were isolated. Restriction analyses and partial sequencing showed that all cDNA clones belong to the same cDNA class. The longest cDNA, of 2,258 bp, represents an almost full-length transcript compared with the transcript size of 2.4 kb from the Northern blot analysis (see Fig. 3A). The cDNA contains a short open reading frame from nucleotides 571 to 840. The predicted DDLC1 protein is 89 amino acids long, with a calculated molecular mass of 10 kDa (Fig. 2A). Database searches revealed a high degree of sequence similarity (92%) between the *D. melanogaster* DDLC1 protein and the 8-kDa dynein light chain from *C. reinhardtii* (17) (Fig. 2B). This 91-amino-acid peptide was isolated as a component of the outer-arm dynein from the flagellum of the unicellular algae. The high degree of sequence identity between DDLC1 and the 8-kDa outer-arm dynein light chain suggests that the *ddlc1* gene product is the fly homolog of the *Chlamydomonas* dynein light chain.

**The 2.4-kb *ddlc1* transcript is expressed ubiquitously throughout development.** The temporal expression of the *ddlc1* gene was assessed by Northern hybridization with poly(A)$^+$ RNA prepared from various developmental stages and the 2.3-kb cDNA as probe. The results shown in Fig. 3A indicate that the 2.4-kb *ddlc1* mRNA is detected at high levels in all stages of development, i.e., in the embryo, larva, pupa, and adult body and head. In addition to the major, 2.4-kb *ddlc1* mRNA, a second developmentally regulated, 4.5-kb transcript is seen. It can be detected weakly during late (12- to 24-h) embryogenesis and in the pupa. High levels of the 4.5-kb transcript could be detected only in the adult head (Fig. 3A). Upon longer exposure, low-level expression was detectable in larvae. The 4.5-kb mRNA was not detectable during early embryogenesis (0 to 12 h) or in the adult body.

The temporal and spatial distribution pattern of the *ddlc1* transcripts in the adult ovary and in embryos was assessed by whole-mount RNA in situ hybridization with the 2.3-kb cDNA as probe (Fig. 3B to E). Figure 3B shows a particularly strong *ddlc1* staining in nurse cells at all stages of egg chamber development. A strong staining in the oocyte and in follicle cells can be detected at stage 10 of oogenesis and continues until the mature egg is formed. A weak ubiquitous staining is detectable in the embryos up to stage 9 of embryogenesis, most probably indicating maternally contributed *ddlc1* transcript (Fig. 3C). The staining intensity is significantly increased in stage 10 embryos (Fig. 3D), probably indicating the onset of the zygotic *ddlc1* expression. The level of general staining decreases slightly after stage 10, and staining is enriched in the central nervous system and some cells of the peripheral nervous system (chordotonal organs) from stage 14 onward (Fig. 3E).

The analysis of the spatial expression of the *ddlc1* gene with

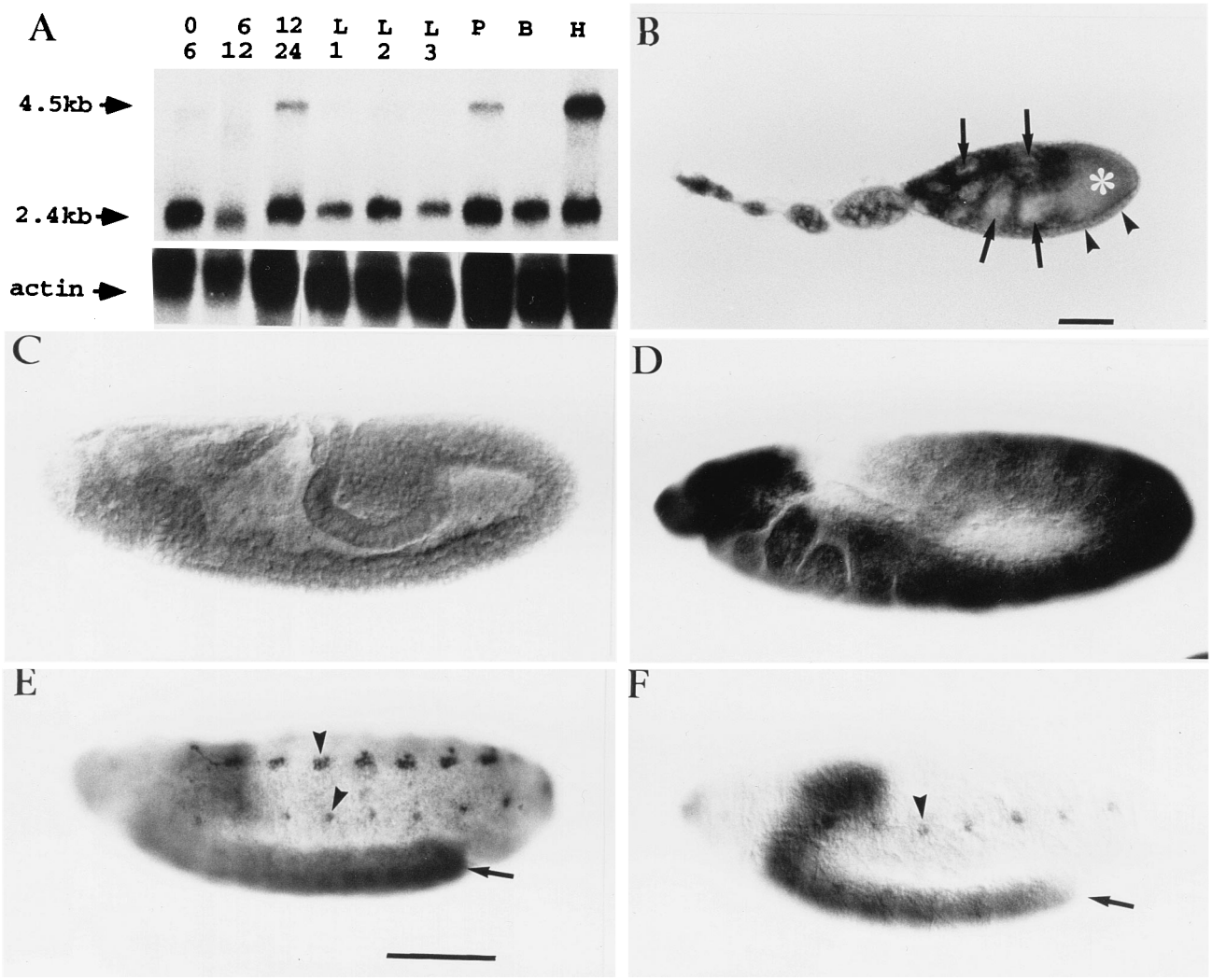


FIG. 3. *ddlc1* transcription during development, in the ovary and in the embryo. (A) Developmental profile of *ddlc1* transcription. A Northern blot probed with 2.3-kb *ddlc1* [$^{32}$P]cDNA is shown. Each lane contains 2 μg of poly(A)$^+$ RNA prepared from embryonic stages (0 to 6 h, 6 to 12 h, and 12 to 24 h after egg deposition), larval stages (L1, first instar; L2, second instar; L3, third instar), pupae (P), adult body (B), and adult head (H). The arrows indicate the ubiquitous 2.4-kb transcript and the developmentally regulated 4.5-kb mRNA. The blot was reprobed with actin to demonstrate approximately equal loading of the RNAs in the different lanes (lower panel). (B to F) Spatial distribution of *ddlc1* transcription. Whole-mount RNA in situ hybridizations of ovaries (B) and embryos (C to F) are shown. The samples (B to E) were hybridized with digoxigenin-labelled 2.3-kb cDNA *ddlc1* antisense probe (see Materials and Methods). A sense probe was used as a negative control (data not shown). (B) A single ovariole containing egg chambers at various stages of development. The staining is ubiquitous. Note the strong expression in the nurse cells (arrows), follicle cells (arrowheads), and oocyte (asterisk) at stage 10 of oogenesis (staging of egg chamber development is that of Spradling [36]). (C to E) Embryos at various stages probed with 2.3-kb cDNA antisense probe. (C) Weak ubiquitous staining of a stage 9 embryo. (D) Strong ubiquitous staining of a stage 10 embryo. (E) Stage 16 embryo, showing enriched staining in the cells of the central nervous system (arrow) and in the neurons of the chordotonal organs (arrowheads) in addition to ubiquitous staining. (F) Stage 16 embryo probed with an antisense probe generated from genomic DNA fragment 3 which is specific for the 4.5-kb *ddlc1* mRNA (Fig. 1). The staining is restricted to the central nervous system (arrow) and the neurons of the chordotonal organs (arrowhead). The pattern matches the neural enrichment of the staining seen in panel E with the 2.3-kb cDNA as probe (see the text). The bottom row of chordotonal cells seen in panel E is out of focus in panel F. All embryos are shown with the anterior to the left and the ventral side down. (C, D, and F) Lateral views. (E) Ventrolateral view. Bars, 100 μm.

the 2.3-kb cDNA (which represents the 2.4-kb mRNA) as a probe does not distinguish between the major, 2.4-kb mRNA and the developmentally regulated 4.5-kb mRNA (see above). To differentiate the expression of the two mRNAs spatially, the transcription pattern of the developmentally regulated 4.5-kb transcript was determined with a genomic probe specific to the 4.5-kb *ddlc1* mRNA (Fig. 1 legend) (see Materials and Methods) in whole-mount RNA in situ experiments. No expression of the 4.5-kb transcript was detectable in ovaries (results not shown). In embryos, the probe specific to the 4.5-kb mRNA produced a tissue-specific staining in the late central nervous system and some cells of the peripheral nervous system (chordotonal organs) from stage 14 onward (Fig. 3F). No early ubiquitous staining was observed. Since the 4.5-kb transcript is not expressed in ovaries and shows only a neural tissue-specific expression in late embryos, it can be concluded that the ubiquitous *ddlc1* staining detected with the 2.3-kb cDNA probe in these tissues is due to the expression of the major, 2.4-kb transcript. This conclusion is consistent with the developmental Northern blot analysis (Fig. 3A) that shows that the 2.4-kb mRNA is detected at high levels throughout development whereas the 4.5-kb mRNA is not detectable in the body and

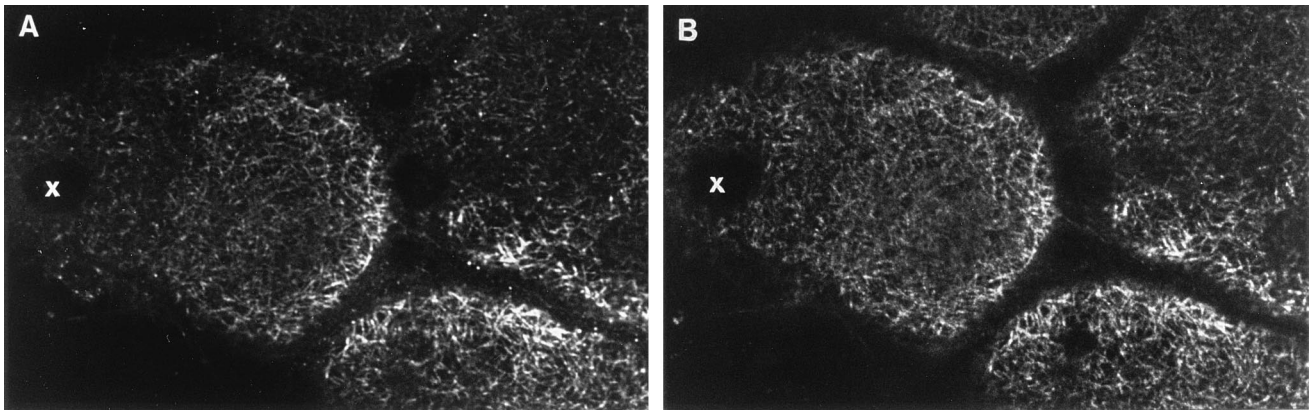


FIG. 4. Cytoplasmic localization and tubulin colocalization of the DDLC1 protein. Whole-mount preparations of *Drosophila* ovaries were double labelled with mouse anti-DDLC1 antibody (A) and rat anti-α-tubulin antibody (B) to determine the subcellular localization of DDLC1. Nurse cells are shown. The DDLC1 antigen is localized in the cytoplasm (A) and colocalizes with the tubulin staining (B), suggesting that DDLC1 is associated with the microtubules. The mouse antiserum labelling was visualized with anti-mouse-conjugated fluorescein isothiocyanate antibody, and the rat antiserum labelling was visualized with anti-rat-conjugated rhodamine isothiocyanate antibody. The nurse cell nucleus is indicated by X. As a control for DDLC1 localization, the anti-DDLC1 antibody was preincubated against the DDLC1 peptide antigen. The preincubation eliminated the staining (not shown).

early embryos. The neural tissue-specific expression pattern of the 4.5-kb mRNA in late embryos matches the neural tissue-enriched staining shown by the 2.3-kb cDNA probe. Since the 2.3-kb cDNA hybridizes to both the 2.4- and 4.5-kb mRNAs, the neural enrichment seen with the 2.3-kb cDNA probe may be due to the expression of the 4.5-kb mRNA in this tissue and not to an enrichment of the ubiquitously expressed 2.4-kb mRNA. Taken together, the preliminary analyses of the 4.5-kb *ddlc1* transcript presented in this report suggest that the *ddlc1* gene encodes, in addition to the ubiquitously expressed 2.4-kb mRNA, a neural tissue-specific transcript. This conclusion is supported by the high level of 4.5-kb mRNA detected in RNA preparations from adult heads (Fig. 3A). Whether the neural *ddlc1* transcript encodes a neural tissue-specific DDLC1 protein version and what functional role it plays in the nervous system remain to be seen. The 4.5-kb transcript clearly does not play a role in the genetic and phenotypic analyses of the *ddlc1* gene presented below because it is not expressed in early embryos or the adult body or ovaries. Therefore, this report focuses exclusively on the molecular and functional characterization of the ubiquitously expressed major, 2.4-kb *ddlc1* transcript and its encoded protein, DDLC1.

**The DDLC1 protein encoded by the major, 2.4-kb *ddlc1* transcript is cytoplasmically localized and colocalizes with tubulin.** The ubiquitous expression of the major, 2.4-kb mRNA, e.g., in embryos lacking motile cilia and flagella (16, 35), implies that the fly DDLC1 protein must be localized in the cytoplasm as opposed to the flagellum, where the *C. reinhardtii* outer-arm dynein light chain is found (17). Hence, DDLC1 is apparently a cytoplasmic dynein light-chain homolog of the axonemal dynein light chain of the algae. To provide direct evidence for the cytoplasmic localization of the DDLC1 protein, polyclonal antibodies were raised against a DDLC1 peptide and the subcellular localization was determined. The results shown in Fig. 4A demonstrate that the DDLC1 protein is localized in the cytoplasm. The cytoplasmic dynein heavy chain from *D. melanogaster* is found in association with multiple microtubule arrays (13). To determine whether the DDLC1 protein is associated with microtubules, a double-labelling experiment with anti-DDLC1 antibody and anti-tubulin antibody was carried out. Comparison of the anti-DDLC1 staining shown in Fig. 4A with the anti-tubulin staining in Fig. 4B shows that the two proteins colocalize. The staining of the DDLC1 protein in embryos and ovaries is, like the RNA in situ staining, essentially ubiquitous (results not shown).

Taken together, the immunocytochemical analyses show that the DDLC1 protein encoded by the ubiquitous 2.4-kb *ddlc1* mRNA is localized in the cytoplasm. Its association with microtubules is similar to the subcellular localization described for the dynein heavy-chain subunit of the cytoplasmic dynein complex (13).

**Partial loss of *ddlc1* function causes pleiotropic morphogenetic defects in the adult fly.** The original *ddlc1* mutation ($ddlc1^{ins1}$) is a viable P-element insertion ≈40 bp upstream of the *ddlc1* transcription unit and causes recessive female sterility. In addition to being sterile, homozygous $ddlc1^{ins1}$ females (and hemizygous $ddlc1^{ins1}$ males) show various morphological defects. Their wings show a small delta at the end of the wing veins, and the bristles are thinner than in the wild type (data not shown). Analysis of the ovaries revealed that the ovarioles and egg chambers are disorganized to various degrees. This ovarian defect obviously accounts for the female sterility. Similar phenotypes are associated with two other independently isolated P-element alleles, $ddlc1^{ins2}$ and $ddlc1^{ins3}$, respectively (see Materials and Methods). The isolation of three independent *ddlc1* P-element alleles associated with similar phenotypes, together with the fact that $ddlc1^{ins1}$ is inserted only ≈40 bp upstream of the transcriptional start site of the 2.4-kb transcript, i.e., into the putative promoter region of the *ddlc1* gene, strongly suggests that the gene affected by the P elements is the *ddlc1* gene and not some other, unknown neighboring gene. The conclusion that the *ddlc1* gene is indeed the gene affected by the P-element insertions is further supported by the results of allelic combination experiments. The ovarian disorganization is more severe when the P-insertion $ddlc1^{ins1}$ allele is heterozygous with the *ddlc1* deletion alleles (in $ddlc1^{ins1}$/$ddlc1^{exc3}$ and $ddlc1^{ins1}$/$ddlc1^{exc6}$ flies [Fig. 1]), indicating that the P-element insertion allele is a partial-loss-of-function mutation of the *ddlc1* gene. Precise excisions of the P element of the $ddlc1^{ins1}$ allele cause all adult defects to revert, confirming that these abnormalities are caused by the P element.

To analyze the ovarian phenotype in more detail, mutant ovaries were stained with phalloidin to visualize the actin cytoskeleton and with the DNA-staining dye DAPI to show the nuclei. The left column in Fig. 5 shows wild-type ovaries com-

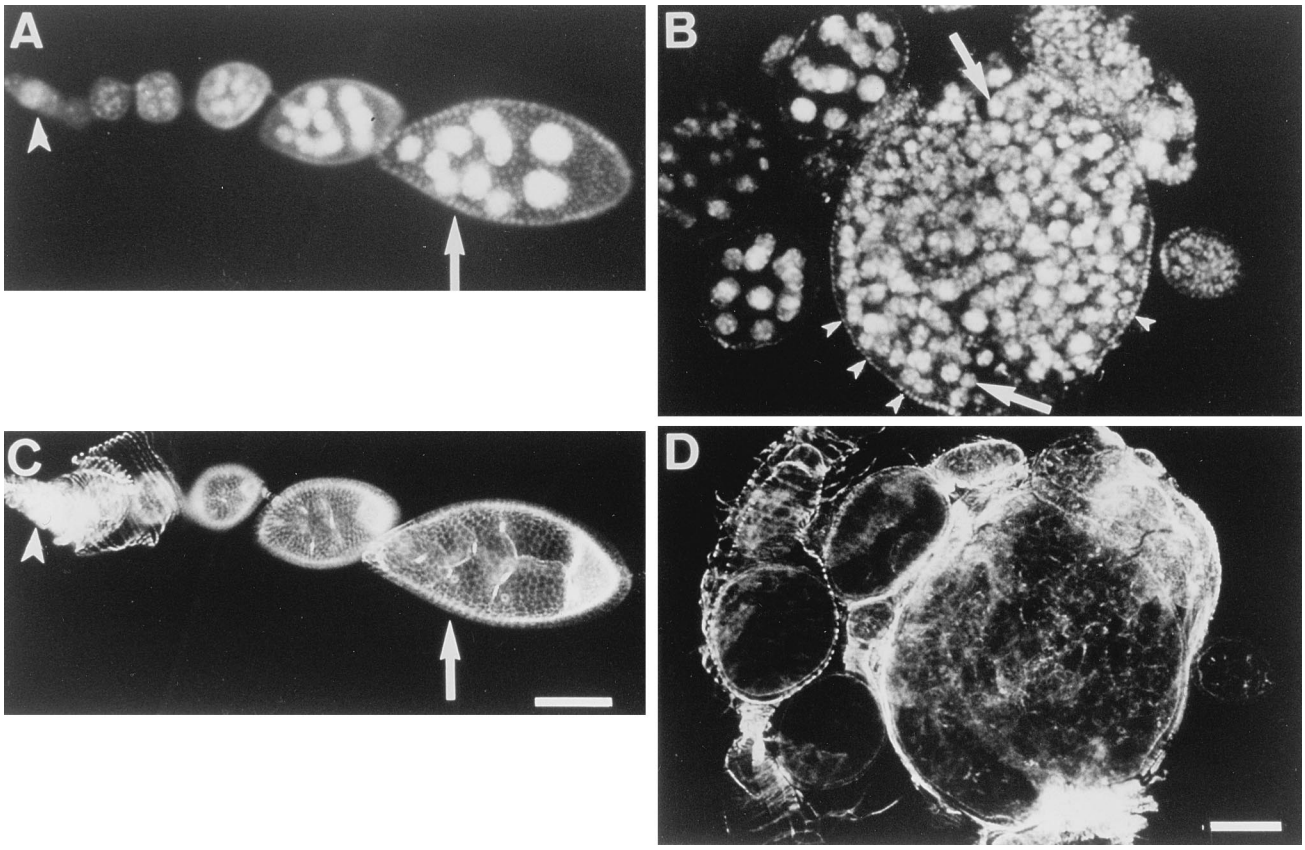


FIG. 5. Ovarian phenotypes caused by the partial loss of *ddlc1* function. Ovarioles and egg chambers of the wild type (left column) and of homozygous P-element insertion animals ($ddlc1^{ins1}/ddlc1^{ins1}$, right column) are shown. (A and B) Staining with DAPI to visualize the nuclei. (C to J) Staining with phalloidin to reveal the actin cytoskeleton (see Materials and Methods). (A and C) Wild-type ovarioles. The arrowheads indicate the germarium, and the arrows indicate a stage 6 egg chamber. A string of egg chambers at various stages of development are present in between. The egg chambers are connected by stalk cells. Bar, 100 μm. (B and D) Mutant ovarioles. Fused egg chambers with a large number of nurse cells (arrows) and follicle cells (arrowheads) are observed. Bar, 100 μm. (E) Stage 2 egg chamber (arrow) budding from a wild-type germarium. The arrowhead indicates the syncytium surrounded by follicle cells. (F) Abnormally large "egg chamber" which has failed to bud off from a mutant germarium correctly. The arrowhead indicates ring canals, and the arrow indicates follicle cells. Bar, 50 μm. (G and H) Wild-type (stage 6) and mutant egg chambers, respectively, focused on the follicle cells. Note the regular arrangement of the follicle cells in the wild type (G) and the disorganization (arrow) in the mutant (H). Bar, 50 μm. (I and J) Wild-type (stage 6) and mutant egg chambers, respectively, focused on the nurse cells. Nurse cells (n), follicle cells (arrow), oocyte (asterisk), and the ring canals (arrowheads) are indicated. Bar, 50 μm.

posed of ovarioles, bundles of developmentally ordered egg chambers (Fig. 5A and C). Each egg chamber supports the development of a single oocyte. Oogenesis is initiated at the germarium (Fig. 5A and C) by a stem cell division that produces a cystoblast and regenerates a stem cell. The cystoblast proceeds through mitotic divisions to produce an egg chamber of 16 germ line cells that will differentiate to form the single oocyte and 15 nurse cells (Fig. 5I). During oogenesis, the nurse cells synthesize maternal components for transport to the oocyte. Cytokinesis is incomplete at each of the cystoblast divisions, which leaves the 16 germ line cells interconnected by large cytoplasmic bridges, called ring canals (Fig. 5I). When the egg chamber buds off from the germarium, it is surrounded by a layer of follicle cells (Fig. 5E, G, and I) (see reference 36 for a review).

The defects found in homozygous mutant animals ($ddlc1^{ins1}/ddlc1^{ins1}$) are variable, and a wide range of abnormal ovarioles and egg chambers can be observed (Fig. 5, right column). Figure 5B and D shows a severe example of a completely disorganized mutant ovariole. The observed large bags of cells probably result from a fusion of several egg chambers during the budding process from the germarium (Fig. 5F). Often, the egg chambers bud off from the germarium apparently correctly but fail to differentiate properly afterward. Figure 5H and J shows drastically disorganized egg chambers in which the cellular morphology of the nurse cells and follicle cells, respectively, is strongly affected. The severity of the ovarian phenotype is, however, variable, and fully formed eggs are sometimes found in mutant ovarioles. However, the mutant females are completely sterile.

Taken together, the pleiotropic defects in bristle, wing, and egg formation show that a partial loss of *ddlc1* gene function affects morphogenesis and differentiation as well as cell morphology.

**Total loss of *ddlc1* function is lethal and causes embryonic degeneration and widespread apoptotic cell death.** Two deletion alleles of *ddlc1* were generated by mobilization of the P element in the $ddlc1^{ins1}$ chromosome (Fig. 1) (see Materials and Methods). Both *ddlc1* deletions start at the P-element insertion site and remove either all ($ddlc1^{exc3}$) or part ($ddlc1^{exc6}$) of the *ddlc1* transcription unit specifying the ubiquitous 2.4-kb *ddlc1* transcript (Fig. 1). Both *ddlc1* deletion alleles cause recessive lethality. Homozygous $ddlc1^{exc}$ flies were never observed, and the $ddlc1^{exc}$ alleles were kept over FM7c balancer chromosomes. Their lethalities map to the same complementation group, and both mutations also fail to com-

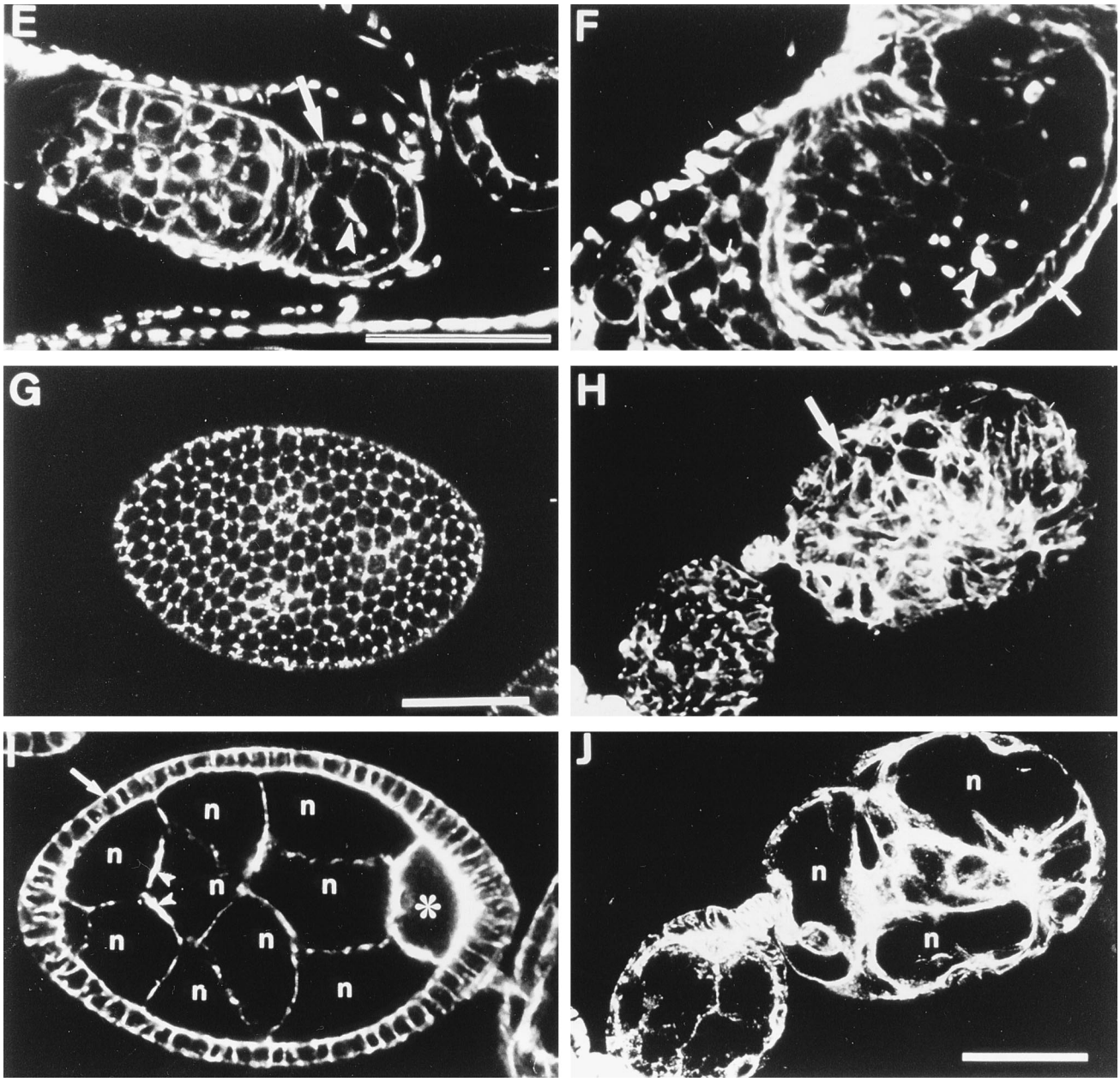


FIG. 5—*Continued.*

plement the *ddlc1*$^{ins}$ alleles for female sterility. The severity of the ovarian disorder in flies containing the P-element insertion *ddlc1* allele *ddlc1*$^{ins1}$ combined with the deletion alleles *ddlc1*$^{exc3}$ and *ddlc1*$^{exc6}$ (*ddlc1*$^{ins1}$/*ddlc1*$^{exc3}$ and *ddlc1*$^{ins1}$/*ddlc1*$^{exc6}$) is similar to the severity of the ovarian disorganization found in flies containing the *ddlc1*$^{ins1}$ allele over the deficiency Df(1)ovoG6, which removes large parts of the chromosome surrounding the *ddlc1* gene [*ddlc1*$^{ins1}$/Df(1)ovoG6]. These results indicate that both *ddlc1*$^{exc3}$ and *ddlc1*$^{exc6}$ are total-loss-of-function alleles.

To determine the phase of lethality of homozygous *ddlc1*$^{exc3}$ and *ddlc1*$^{exc6}$ animals, parents heterozygous for the respective *ddlc1*$^{exc}$ mutation were mated, 500 eggs from each cross were collected, and their development to larvae was scored. A total of 27% *ddlc1*$^{exc3}$ and 25% *ddlc1*$^{exc6}$ eggs did not develop to larvae; i.e., they died as embryos. The control experiment to determine the lethality caused by the (FM7c) genetic background showed that 4% of these "wild-type" eggs fail to develop to larvae (8 of 200 eggs). Hence, both the *ddlc1*$^{exc}$ alleles cause death, predominantly during embryogenesis.

To characterize the embryonic lethality in more detail, parents heterozygous for the respective *ddlc1*$^{exc}$ mutations were mated and 2-h embryo collections (1,300 eggs each) were fixed immediately or allowed to develop for 1, 2, or 4 h, respectively, before being fixed. Hemizygous mutant embryos (*ddlc1*$^{exc}$/Y) were identified by anti-β-galactosidase staining. The FM7c balancer chromosome contains an *ftz-lacZ* marker gene. Embryos heterozygous and homozygous for FM7c stain for β-galactosidase, whereas mutant *ddlc1*$^{exc}$ embryos can be identified by their lack of staining. To characterize the phenotype of mutant

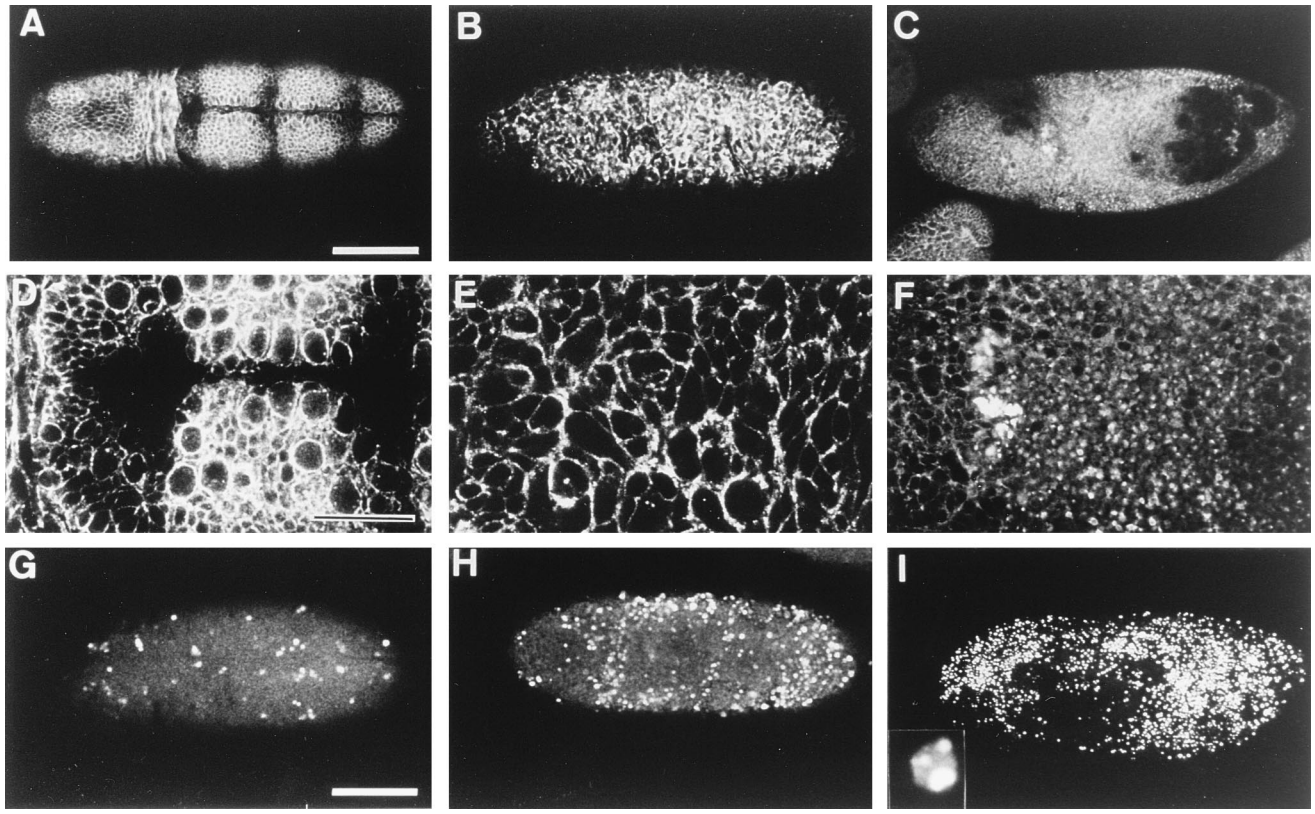


FIG. 6. Embryonic phenotypes caused by the total loss of *ddlc1* function. Stage 10 embryos of the wild-type (left column) and two $ddlc1^{exc3}$ mutant embryos showing different degrees of degeneration (middle and right columns) are presented. (A to F) Embryos stained with phalloidin. (D to F) Higher magnifications of panels A to C to emphasize the regular cellular structure of the wild-type embryo (A and D) and the disorganized cellular morphology (B and E) and cytoplasmic condensation (C and F) in degenerating mutant embryos. Bars, 100 μm (A to C) and 50 μm (D to F). (G to I) Embryos stained with terminal transferase and biotin-dUTP (TUNEL) to visualize nuclear DNA fragmentation in situ. (G) Wild-type embryo with a few apoptotic nuclei. (H and I) Massive nuclear staining in degenerating mutant embryos, indicating massive apoptotic cell death. Bar, 100 μm. The inset in panel I shows higher magnification of a fragmented mutant nucleus stained with YPRO-I. $ddlc1^{exc6}$ mutant embryos show similar results.

embryos, embryos were costained with phalloidin to visualize the actin cytoskeleton and with the DNA-labelling dye YPRO-I to show the nuclei. The analyses revealed that up to stage 10, each stage contains about 25% β-galactosidase-negative (mutant) embryos, indicating that $ddlc1^{exc}$ mutant embryos develop normally until stage 10 (staging according to reference 5), i.e., 4.20 to 5.20 h of embryogenesis. In later stages, hardly any β-galactosidase-negative embryos were detected, indicating that most mutant embryos do not develop beyond stage 10. The phalloidin and YPRO-I staining shows that most β-galactosidase-negative embryos stop developing properly and degenerate after stage 10. Figure 6 shows phalloidin staining of a wild-type stage 10 embryo (Fig. 6A and D) and of mutant embryos at different stages of degeneration (Fig. 6B and E and C and F). It clearly shows that the actin cytoskeleton in mutant embryos becomes severely disorganized (Fig. 6B and E) and finally the cytoplasm becomes condensed and fragmented (Fig. 6C and F). The YPRO-I staining revealed nuclear condensation and fragmentation in the dying cells, an indication of apoptotic cell death (Fig. 6I, inset). Apoptotic cell death is usually accompanied by DNA fragmentation (see references 37, 38, and 47 for reviews). To test in situ whether this characteristic feature of programmed cell death can be detected in the dying embryonic cells, a TUNEL staining (see Materials and Methods), which detects DNA degradation, was carried out. Embryo collections and identification of hemizygous mutants were done as described above. The analysis showed that before stage 10, no significant TUNEL staining was detectable in mutant embryos. At stage 10, widespread massive TUNEL staining was observed. Figure 6G shows a wild-type stage 10 embryo, and mutant embryos at different stages of degeneration are shown in Fig. 6H and I. This clearly demonstrates that most of the nuclei in the dying mutant embryos contain fragmented genomic DNA.

The lethal phenotype of total-loss-of-function alleles shows that *ddlc1* function is essential. The mutant animals die predominantly as embryos at stage 10, the probable onset of zygotic *ddlc1* expression. The embryos degenerate and show a severely disorganized actin cytoskeleton. Many cells show condensation and fragmentation of cytoplasm as well as degradation of genomic DNA, indications of programmed cell death.

***hdlc1*/HDLC1 is highly conserved, cytoplasmically localized, and ubiquitously expressed and maps to 14q24.** Database searches revealed a high degree of sequence similarity (94%) between the *D. melanogaster* DDLC1 protein and the hypothetical gene product T26A5.9 from *Caenorhabditis elegans* (chromosome III) (46) (Fig. 2B). Since nematodes have no motile cilia or flagella at any stage of their life cycle (6), this suggests that T26A5.9 encodes a homolog (CDLC1) of the cytoplasmic DDLC1 protein of the fly (see also reference 17 for a discussion). The high degree of conservation of the DLC1 proteins in arthropods and nematodes suggested that a cytoplasmic type 1 dynein light chain might be present in all metazoans. To isolate a human homolog of DDLC1/CDLC1, oli-

gonucleotide primers were designed by reverse translation of conserved N- and C-terminal sequences of the *D. melanogaster* and *C. elegans* DLC1 proteins and PCR was used to obtain a 300-bp human *hdlc1* probe (see Materials and Methods). Two overlapping cDNAs were isolated, and the longest cDNA clone (643 bp) was sequenced. It contains an open reading frame of 89 amino acids from nucleotides 94 to 363 and a consensus poly(A) sequence 18 bp from the 3′ end. The deduced protein (HDLC1) has 92% identity to the *C. elegans* CDLC1 and 94% identity to the *D. melanogaster* DDLC1, respectively (Fig. 2B).

The expression of the *hdlc1* transcript was assessed by Northern hybridization with poly(A)$^+$ RNA prepared from various adult tissues. When *hdlc1* cDNA was used as a probe, a major 0.7-kb and a minor 2.5-kb transcript were detected in all tested tissues, suggesting ubiquitous expression of *hdlc1* in adults (Fig. 7A).

To provide evidence for the cytoplasmic localization of the HDLC1 protein, transfection studies were carried out. HDLC1 was tagged with the MYC epitope at its N and C termini and cloned into an expression vector (see Materials and Methods). Thus, the plasmids p-Nmyc-hdlc1 and p-Cmyc-hdlc1 were generated. Cos cells were transfected, and the subcellular localization was determined. Both the NMYC-HDLC1 and CMYC-HDLC1 proteins are localized in the cytoplasm (Fig. 7B and legend). Taken together, the cloning of *hdlc1* demonstrates that a highly conserved human homolog of the fly DDLC1 protein exists. Like the fly gene, *hdlc1* is ubiquitously expressed, and the HDLC1 protein is cytoplasmically localized.

Because of the drastic defects of mutations in the fly homolog of the *hdlc1* gene, defects in the human gene might be expected to result in severe disease states. To allow investigation of a possible role of the *hdlc1* gene in inherited disorders, the chromosomal location of *hdlc1* was determined. For this purpose, a human P1 clone was isolated with *hdlc1* cDNA as probe and used for fluorescence in situ hybridization (see Materials and Methods). *hdlc1* is localized to chromosome 14q24. The human cytoplasmic dynein heavy chain was mapped to 14q (24).

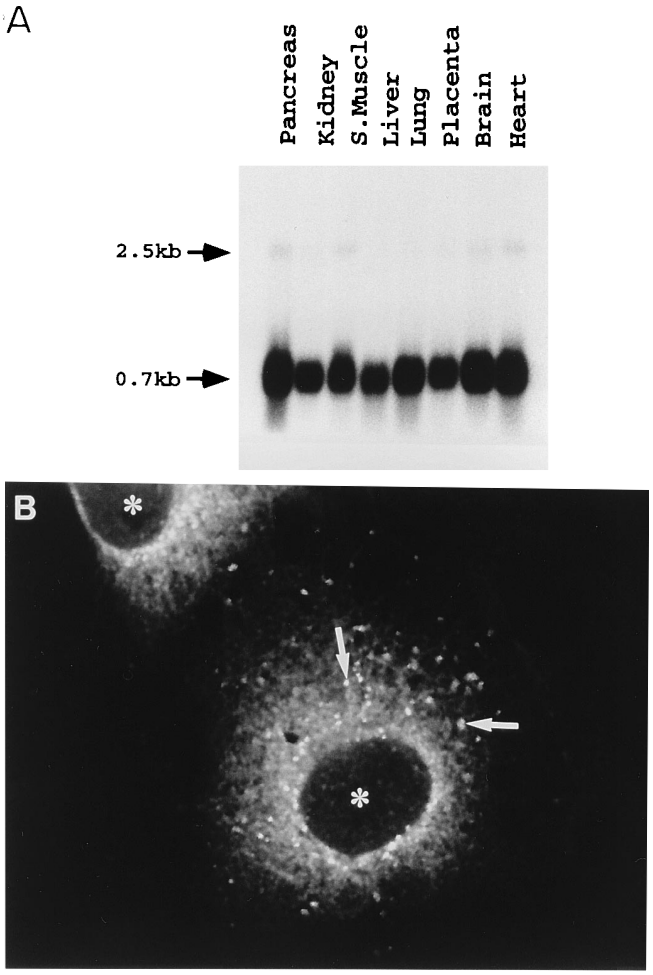


FIG. 7. *hdlc1* expression in adult humans and subcellular HDLC1 localization in Cos cells. (A) Transcription of the human *hdlc1* gene in different adult tissues. A Northern blot probed with *hdlc1* [$^{32}$P]cDNA is shown. Each lane contained 2 μg of poly(A)$^+$ RNA. The arrows indicate the 2.5-kb (upper) and 0.7-kb (lower) transcripts, respectively. S.Muscle, skeletal muscle. (B) Cos cells that had been transfected with p-Cmyc-hdlc1 are shown. This plasmid contains a C-terminally tagged *hdlc1* under the control of the human cytomegalovirus promoter (see Materials and Methods). The cells were grown on coverslips, fixed, and permeabilized prior to being probed with anti-MYC antibody and visualized by indirect immunofluorescence microscopy. CMYC-HDLC1 protein is localized in the cytoplasm. The staining is punctated (arrows). The nucleus is indicated by an asterisk. Transfection experiments with p-Nmyc-hdlc1, in which HDLC1 contains a N-terminal myc tag, show the same results (not shown).

## DISCUSSION

We report here the molecular and genetic characterization of the first cytoplasmic dynein light-chain gene from *D. melanogaster* and identification of its homolog in humans. These animal DLC1 proteins are highly conserved and ubiquitously expressed cytoplasmic homologs of the 8-kDa axonemal outer-arm dynein light chain from *C. reinhardtii*. For *D. melanogaster*, we show that partial-loss-of-function *ddlc1* alleles cause pleiotropic morphological defects in adults. Total-loss-of-function alleles are lethal and cause embryonic degeneration and widespread apoptotic cell death.

**Deduced DLC1 proteins, their expression, and their subcellular localization.** The DLC1 proteins from arthropods, nematodes and vertebrates are highly conserved. All three proteins isolated from *D. melanogaster*, *Caenorhabditis elegans* and humans are 89 amino acids long and 91% identical in their amino acid sequence. All amino acid differences between the various animal DLC1s but one (codon 2) are conservative exchanges. The strong conservation of the DLC1 sequence suggests that the DLC1 molecule is under strong selective pressure, indicating that the protein plays an important functional role.

*dlc1* expression patterns were determined for *D. melanogaster* and humans. In *D. melanogaster*, the *ddlc1* transcript is found at high levels throughout development, i.e., in the embryo, larva, pupa, and adult fly. The expression analysis in the embryo and ovary indicates that *ddlc1* expression is not only temporally but also spatially ubiquitous. The human Northern blot analysis shows a similar result. *hdlc1* is expressed in all adult tissues. Cytoplasmic localization could be demonstrated directly for the *Drosophila* DLC1 protein with polyclonal antibody raised against the fly peptide. Transfection studies provided evidence that the human DLC1 protein is also localized in the cytoplasm. The ubiquitous expression—together with the wide distribution across all metazoan evolutionary boundaries—suggests that the DLC1 protein is part of the fundamental cytoplasmic cellular machinery.

**Implications of the DLC1 homology to the axonemal 8-kDa dynein light chain of *C. reinhardtii*.** The cytoplasmic DLC1s show a striking similarity to the flagellar 8-kDa dynein light chain from *C. reinhardtii*. This 8-kDa peptide is a component of the outer arm of the flagellar (axonemal) dynein (17). The high

degree of sequence identity suggests that the animal DLC1 is a cytoplasmic homology of the axonemal 8-kDa dynein light chain from the *Chlamydomonas* flagellum. Biochemical analyses by King (16a) showed directly that the animal DLC1 is a previously unsuspected component of highly purified bovine cytoplasmic dynein.

Axonemal dynein light chains have been implicated in the initiation of sperm motility (39) and the rate of dynein-mediated microtubule translocation in vitro (2). However, essentially nothing more is known about the function of any dynein light chain. Interestingly, the *Chlamydomonas* 8-kDa outer-arm dynein light chain is associated with the intermediate chains IC78 and IC69 (18) located at the basal domain of the axonemal dynein (19). The axonemal intermediate chains have homologs, IC74, in cytoplasmic dyneins which are also thought to be located at the base of the cytoplasmic dynein complex (23, 25, 45). Because of the interaction of the axonemal 8-kDa dynein light chain with axonemal intermediate chains IC78 and IC69, one could conclude, by analogy, that the highly homologous cytoplasmic DLC1s might interact with the cytoplasmic intermediate-chain homologs. This interaction would position the DLC1 at the basal domain of the cytoplasmic dynein, which is proposed to be involved in the targeting of the dynein complex within the cell (25).

**Implications of the *ddlc1* phenotypes in *D. melanogaster*.** Three independent P-element-induced partial-loss-of-function alleles cause pleiotropic morphogenetic defects in the adult wings, bristles, and ovaries. The ovarian defects were analyzed in some detail and show a wide range of disorganization of ovarioles and egg chambers. These morphological abnormalities are always associated with a loss of cellular shape and structure as visualized by a disorganization of the actin cytoskeleton. These results indicate that *ddlc1* activity is required for proper morphogenesis as well as normal cellular morphology and differentiation.

Two total-loss-of-function alleles, resulting from the partial or complete deletion of the *ddlc1* transcription unit, cause lethality, predominantly in the embryonic phase. A large proportion of the embryos stop developing properly and degenerate after stage 10, the stage at which probably the zygotic expression of the 2.4-kb *ddlc1* transcript begins. The cells in the degenerating embryos show severely disordered cellular architecture as visualized by actin staining. Widespread cell death is observed, showing features associated with programmed cell death, namely, cytoplasmic and nuclear condensation and genomic DNA fragmentation (see references 37 and 47 for reviews). These results show that *ddlc1* function is required for proper embryogenesis and differentiation. The observed widespread embryonic cell death suggests that *ddlc1* function might be essential for many cells during development. The failure to recover homozygous total-loss-of-function cell clones in adult somatic tissue by genetic mosaic experiments indicates that *ddlc1* function might be required for cell viability (29a). The *Drosophila Glued* gene (28), which encodes the fly homolog of dynactin (15), a protein involved in stimulating dynein-dependent vesicle transport (11), is thought to have an essential function for cell viability (12).

How can these in vivo functions of the *ddlc1* gene, namely, its requirement for proper morphogenesis, cell architecture, and differentiation, as well as a possible role in cell viability during development, be related to the potential cell-biological roles of the DDLC1 molecule? DDLC1 is a ubiquitous cytoplasmic homolog of the *Chlamydomonas* 8-kDa light-chain subunit of the axonemal dynein. Therefore, the DDLC1 protein most probably acts as a subunit of the cytoplasmic dynein and is thus involved in some aspects of dynein-related intracellular transport and motility. However, this does not exclude the possibility that DDLC1 is involved in some (unknown) nonmotor functions of dynein or that it plays some non-dynein-related roles. Although it is thought that cytoplasmic dynein is involved in organelle transport and localization and might play a role in chromosomal movement during mitosis, the repertoire of cellular functions involving dynein is poorly understood. Other roles involving microtubulus-associated movements within the cell have been considered (see references 9 and 14 for reviews). The cells of the mutant ovaries, as well as those of the mutant embryos, show severely disordered cytoskeletons. Whether this is a direct or indirect effect of the lack of *ddlc1* function remains to be resolved. However, the observed cytoskeletal defects raise the possibility that DDLC1 plays a role in changing or maintaining the spatial distribution of cytoskeletal structures.

In conclusion, this report presents the first molecular characterization of a light-chain subunit of cytoplasmic dynein. The comparative analyses of DLC1 from *D. melanogaster* and humans show that the structure and the ubiquitous expression of this novel cytoplasmic dynein component are conserved in insects and mammals. The genetic analysis of the dynein light-chain gene in *D. melanogaster* presents the first description of mutations in cytoplasmic dynein and their functional consequences in higher eucaryotes. A detailed analysis of the partial- and total-loss-of-function phenotypes of the *Drosophila ddlc1* gene should provide insight into the various functions and modes of action of cytoplasmic DLC1/dynein in vivo. The availability of the human *hdlc1* homolog should facilitate the DLC1/dynein in vitro analysis with the human cell culture system. Furthermore, comprehensive mapping studies of the human *hdlc1* gene should reveal whether it shows linkage with any previously identified genetic syndromes at 14q24.

## ACKNOWLEDGMENTS

We are grateful to Steve King for fruitful discussions on dynein light chains and for communicating results prior to publication. We thank Tang Bor Luen and Hong Wanjin for discussions and help with the myc-tagging experiment. We thank Bernadette Murugasu-Oei and Sami Bahri for comments on the manuscript. We thank all members of our laboratory for encouragement and discussion.

This work was supported by the Institute of Molecular and Cell Biology (IMCB).

## REFERENCES

1. **Ashburner, M.** 1989. *Drosophila*: a laboratory manual. Cold Spring Harbor Laboratory Press, Cold Spring Harbor, N.Y.
2. **Barkalow, K., T. Hamasaki, and P. Satir.** 1994. Regulation of 22S dynein by 29kD light chain. J. Cell Biol. **126:**727–735.
3. **Bier, E., H. Vaessin, S. Shepherd, K. Lee, K. McCall, S. Barbel, L. Ackerman, R. Carretto, T. Uemura, E. Grell, L. Jan, and Y. N. Jan.** 1989. Searching for pattern and mutation in the *Drosophila* genome with a P-lacZ vector. Genes Dev. **3:**1273–1287.
4. **Brown, N. H., and F. C. Kafatos.** 1988. Functional cDNA libraries from *Drosophila* embryos. J. Mol. Biol. **203:**425–437.
5. **Campos-Ortega, J. A., and V. Hartenstein.** 1985. The embryonic development of *Drosophila melanogaster*. Springer-Verlag KG, Berlin.
6. **Chitwood, B. G., and M. B. Chitwood.** 1974. Introduction to nematology. University Park Press, Baltimore.
7. **Cooley, L., and W. E. Theurkauf.** 1994. Cytoskeletal functions during *Drosophila* oogenesis. Science **266:**590–596.
8. **Cooley, L., E. Verheyen, and K. Ayers.** 1992. Chickadee encodes a profilin required for intracellular cytoplasm transport during *Drosophila* oogenesis. Cell **69:**173–184.
9. **Fyrberg, E. A., and L. S. B. Goldstein.** 1990. The *Drosophila* cytoskeleton. Annu. Rev. Cell Biol. **6:**559–596.
10. **Gibbons, I. R., and A. Rowe.** 1965. Dynein: a protein with adenosine triphosphate activity from cilia. Science **149:**424.
11. **Gill, S. R., T. A. Schroer, I. Szilak, E. R. Steuer, M. P. Sheetz, and D. W. Cleveland.** 1991. Dynactin, a conserved, ubiquitously expressed component

of an activator of vesicle motility mediated by cytoplasmic dynein. J. Cell Biol. **115:**1639–1650.
12. **Harte, P. J., and D. R. Kanklel.** 1982. Genetic analysis of mutations at the Glued locus and interacting loci in *Drosophila melanogaster*. Genetics **101:** 477–501.
13. **Hays, T. S., M. E. Porter, M. McGrail, P. Grissom, P. Gosch, M. T. Fuller, and J. R. McIntosh.** 1994. A cytoplasmic dynein motor in *Drosophila*: identification and localisation during embryogenesis. J. Cell Sci. **107:**1557–1569.
14. **Holzbaur, E. L. F., and R. B. Vallee.** 1994. Dyneins: molecular structure and cellular function. Annu. Rev. Cell Biol. **10:**339–372.
15. **Holzbaur, E. L. F., J. A. Hammarback, B. M. Paschal, N. G. Kravit, K. K. Pfister, and R. B. Vallee.** 1991. Homology of a 150K cytoplasmic dynein-associated polypeptide with the *Drosophila* gene Glued. Nature (London) **351:**579–583.
16. **Kiefer, B. I.** 1973. Genetics of sperm development in Drosophila, p. 47–102. *In* F. H. Ruddle (ed.), Genetic mechanisms of development. Academic Press, Inc., New York.
16a. **King, S. M.** Personal communication.
17. **King, S. M., and R. S. Patel-King.** 1995. The M(r) = 8,000 and 11,000 outer arm dynein light chains from *Chlamydomonas* flagella have cytoplasmic homologs. J. Biol. Chem. **270:**11445–11452.
18. **King, S. M., C. G. Wilkerson, and G. B. Witman.** 1991. The Mr 78,000 intermediate chain of *Chlamydomonas* outer arm dynein interacts with alpha-tubulin in situ. J. Biol. Chem. **266:**8401–8407.
19. **King, S. M., and G. B. Witman.** 1990. Localisation of an intermediate chain of outer arm dynein by immunoelectron microscopy. J. Biol. Chem. **265:** 19807–19811.
20. **Li, M., M. McGrail, M. Serr, and T. S. Hays.** 1994. *Drosophila* cytoplasmic dynein, a microtubule motor that is asymmetrically localized in the oocyte. J. Cell Biol. **126:**1475–1494.
21. **Lindsley, D. L., and G. G. Zimm.** 1992. The genome of *Drosophila melanogaster*. Academic Press, Inc., San Diego, Calif.
22. **Low, S. H., B. L. Tang, S. H. Wong, and W. Hong.** 1995. Retardation of a surface protein chimera at the cis Golgi. Biochemistry **34:**5618–5626.
23. **Mitchell, D. R., and Y. Kang.** 1991. Identification of oda6 as a *Chlamydomonas* dynein mutant by rescue with the wild type gene. J. Cell Biol. **113:** 835–842.
24. **Narayan, D., T. Desai, A. Banks, S. R. Patanjali, T. S. Ravikumar, and D. C. Ward.** 1994. Localisation of the human cytoplasmic dynein heavy chain (DNECL) to 14qter by fluorescence in situ hybridization. Genomics **22:** 660–661.
25. **Paschal, B. M., A. Mikami, K. K. Pfister, and R. B. Vallee.** 1992. Homology of the 74kD cytoplasmic dynein subunit with a flagellar dynein polypeptide suggests an intracellular targeting function. J. Cell Biol. **118:**1133–1143.
26. **Paschal, B. M., and R. B. Vallee.** 1987. Retrograde transport by microtubule-associated protein MAP C1. Nature (London) **330:**181–183.
27. **Perrimon, N., J. D. Mohler, L. Engstorm, and A. P. Mahowald.** 1986. X-linked female sterile loci in *Drosophila melanogaster*. Genetics **113:**695–712.
28. **Plough, H. H., and P. T. Ives.** 1935. Induction of mutations by high temperature in *Drosophila*. Genetics **20:**42–69.
29. **Rasmusson, K., M. Serr, J. Gepner, I. Gibboms, and T. S. Hays.** 1994. A family of dynein genes in *Drosophila melanogaster*. Mol. Biol. Cell **5:**45–55.
29a. **Ray, K.** Unpublished results.
30. **Robertson, H. M., C. R. Preston, R. W. Phillips, D. Johnson-Schlitz, W. K. Benz, and W. R. Engels.** 1988. A stable genomic source of P element transposase in *Drosophila melanogaster*. Genetics **119:**75–83.
31. **Salz, H. K.** 1992. The genetic analysis of snf: a Drosophila sex determination gene required foe activation of sex-lethal in both the germline and the soma. Genetics **130:**547–554.
32. **Salz, H. K., T. W. Flickinger, E. Mittendorf, A. Pellicena-Palle, J. P. Petschek, and E. B. Albrecht.** 1994. The *Drosophila* maternal effect locus deadhead encodes a thioredoxin homolog required for female meiosis and early embryonic development. Genetics **136:**1075–1086.
33. **Sambrook, J., E. F. Fritsch, and T. Maniatis.** 1989. Molecular cloning: a laboratory manual, 2nd ed. Cold Spring Harbor Laboratory Press, Cold Spring Harbor, N.Y.
34. **Schüpbach, T., and E. Wieschaus.** 1991. Female sterile mutations on the second chromosome of *Drosophila melanogaster*. II Mutations blocking oogenesis or altering egg morphology. Genetics **129:**1119–1136.
35. **Smith, D.** 1968. Insect cells: their structure and function. R. and R. Clark Ltd., Edinburgh.
36. **Spradling, A. C.** 1993. Developmental genetics of oogenesis, p. 1–70. *In* M. Bate and A. M. Arias (ed.), The development of *Drosophila melanogaster*. Cold Spring Harbor Laboratory Press, Cold Spring Harbor, N.Y.
37. **Steller, H.** 1995. Mechanisms and genes of cellular suicide. Science **267:** 1445–1449.
38. **Steller, H., and M. E. Grether.** 1994. Programmed cell death in *Drosophila*. Neuron **13:**1269–1274.
39. **Stephens, R. E., and G. Prior.** 1992. Dynein from serotonin-activated cilia and flagella: extraction characteristics and distinct sites for cAMP-dependent protein phosphorylation. J. Cell Sci. **103:**999–1012.
40. **Tamkun, J., R. Deuring, M. Scott, M. Kissinger, A. Pattatucci, T. Kaufman, and J. Kennison.** 1992. Brahma: a regulator of *Drosophila* homeotic genes structurally related to the yeast transcriptional activator SNF2/SWI2. Cell **68:** 561–572.
41. **Tautz, D., and C. Pfeifle.** 1989. A non-radioactive in situ hybridization method for the localisation of specific RNAs in *Drosophila* embryos reveals translational control of the segmentation gene hunchback. Chromosoma **98:** 81–85.
42. **Vallee, R. B.** 1993. Molecular analysis of microtubule motor dynein. Proc. Natl. Acad. Sci. USA **90:**8769–8772.
43. **Vallee, R. B., J. S. Wall, B. M. Paschal, and H. S. Shpetner.** 1988. Microtubule-associated protein 1C from brain is a two-headed cytosolic dynein. Nature (London) **332:**561–563.
44. **White, K., M. E. Grether, J. M. Abram, L. Young, K. Farrell, and H. Steller.** 1994. Genetic control of programmed cell death in *Drosophila*. Science **264:** 677–683.
45. **Wilkerson, C. G., S. M. King, A. Koutoulis, G. J. Pazour, and G. B. Witman.** 1995. The 78,000 intermediate chain of *Chlamydomonas* outer arm dynein is a WD-repeat protein required for arm assembly. J. Cell Biol. **129:**169–178.
46. **Wilson, R., R. Ainscough, K. Anderson, C. Baynes, M. Berks, J. Bonfield, J. Burton, M. Connell, T. Copsey, J. Cooper, A. Coulson, M. Craxton, S. Dear, Z. Du, R. Durbin, A. Favello, L. Fulton, A. Gardner, P. Green, T. Hawkins, L. Hillier, M. Jier, L. Johnston, M. Jones, J. Kershaw, J. Kirsten, N. Laister, P. Latreille, J. Lightning, C. Lloyd, A. McMurray, B. Mortimore, M. O'Callaghan, J. Parsons, C. Percy, L. Rifken, A. Roopra, D. Saunders, R. Shownkeen, N. Smaldon, A. Smith, E. Sonnhammer, R. Staden, J. Sulston, J. Thierry-Mieg, K. Thomas, M. Vaudin, K. Vaughan, R. Waterston, A. Watson, L. Weinstock, J. Wilkinson-Sproat, and P. Wohldman.** 1994. 2.2 Mb of contiguous nucleotide sequence from chromosome III of *C. elegans*. Nature (London) **368:**32–38.
47. **Wyllie, A.** 1995. The genetic regulation of apoptosis. Curr. Opin. Genet. Dev. **5:**97–104.
48. **Yang, X., S. Yeo, T. Dick, and W. Chia.** 1993. The role of a *Drosophila* POU homeo domain gene in the specification of neural precursor cell identity in the developing embryonic central nervous system. Genes Dev. **7:**504–516.